

## Effect of Temperature and Creep on Roller Compacted Concrete Dam During the Construction Stages

A. A. Abdulrazeg<sup>1</sup>, J. Noorzai<sup>1,2</sup>, P. Khanehzaei<sup>1</sup>  
M. S. Jaafar<sup>1</sup> and T. A. Mohammed<sup>1</sup>

**Abstract:** Development of temperature rise in massive concrete structure such as a roller compacted concrete dam is attributed to hydration of concrete and environmental boundary conditions. These thermal changes in the material affect the elastic, creep properties of the material, and in turn, the stress fields within the structure. Therefore, the effects of temperature on the properties of RCC materials( elastic, creep) has to be taken into account in order to determine the risk of the thermally induced cracking in these dams. In the present work an attempt has been made to consider the effect of temperature on the elastic and creep properties. A viscoelastic model, including ageing effects and thermal dependent properties is adopted for the concrete. Safety against a crack occurrence over the time is determined using crack criterion factor. The result has shown that, the increase of the elastic modulus has been accelerated duo to the high temperature of hydration at the initial stage, and consequently stresses are increased. The maximum principle stresses increased by 40% in the initial stage.

**Keywords:** FEM; Roller compacted concrete dam; Thermal stress; Creep; crack criterion factor.

### 1 Introduction

The design and construction of roller compacted concrete dams (RCC) involves solving the problem of temperature control. In the recent years, many numerical models have been proposed to predict realistic distribution of temperatures in these types of massive concrete structures particularly during the constructions phases. The proposed numerical models range from low level of the approximate methods to highly accurate levels using the two or three dimensional sophisticated finite element analysis.

---

<sup>1</sup> Civil Eng. Dep. Universiti Putra Malaysia, UPM-Serdang, Malaysia

<sup>2</sup> Institute of advance Technology, Universiti Putra Malaysia, UPM-Serdang, Malaysia

The temperature rising in RCC dams is due to hydration of cement and climatic changes on the convective boundaries. In addition, the quick construction process can induce a high thermal gradient in interior mass and exterior surface of the dam [Noorzaei et al, 2006]. Temperature does not only influence the properties of concrete such as elastic modulus and creep properties, but also induces thermal stresses [Wu and Luna, 2001]. If these thermal stresses, in addition to the tensile stresses resulting from other loads, exceed the tensile strength of RCC, crack will develop in the dam body.

Details steps for performing a complete thermal study for a simple mass concrete dam structure was discussed by Tarto [Tarto and Schrader.(1985)]. In the presented work the incremental construction concept was incorporated into the model by assigning material placement times relative to a common time of origin to each defined mode element. However, approximated air temperature was used in the work. Later on, Saetta presented a finite element procedure for the stress-strain analysis in concrete structures exposed to time-variable environmental conditions. In this study, the authors ignored the effect of the variation of the elastic modulus with time [Saetta et al. 1995].

A simplified thermal and structural analysis of Kinta RCC dam using ANSYS finite element computer program was presented by Crichton. The variation of the elastic modulus with time, creep behavior and simulation of construction process were considered in this study. However, the ambient air temperature is kept constant through the whole year, and the temperature effect on the elastic and creep properties has been ignored [Crichton et. al. 1999]. Jaafar dealt with the development of a finite element modeling based computer code for the determination of temperatures within the dam body. The finite element code was then applied to the real full-scale problem to determine the impact of the placement schedule on the thermal response of roller compacted concrete dam. In the presented study only thermal analysis was preformed [Jaafar et al, 2007].

A distribution of temperature and stress of the Mianhuatan RCC gravity dam in China was simulated by Zhang. Several factors of RCC affecting dam temperature and stress such as placing process, creep, heat of hydration, effects caused by surrounding temperature were taken into account in the numerical simulation. The main annual air temperature and mean annual river water temperature are used to predict the temperature and stress fields for long-term operation period [Zhang and Zhu.2003].

Noorzaei focused on the development, verification and application of a three-dimensional finite element code for coupled thermal and structural analysis of roller compacted concrete dams. The actual climatic conditions and thermal properties of the materials were considered in the analysis. The structural stress analysis was

performed using the elasto-plastic stress analysis. The studies conclude that, the elasto-plastic analysis can redistribute the state of stresses and produces a more realistic profile of stresses in the dam. However, the time dependent deformations such as; creep and shrinkage have not been reported in their study [Noorzai et al. 2009]

Araujo and Awruch (1998), investigate the cracking phenomena in concrete gravity dams during the construction phase. Stresses due the self weight, thermal gradient, creep and shrinkage are computed taken into account different stages of the construction process. A two dimensional finite element analysis was used in their work during the construction phase. During the analysis, the temperature of the surrounding air was assigned a fixed value which represents the observed mean temperature at the dam site for a period of ten years.

Evidently, roller compacted concrete dams are special structures, because they are constructed in layers, the gravity load is changing with construction process, in addition thermal stress will increase with time as volume of placed concrete is increased. Moreover, each layer has different age, consequently different mechanical, thermal and creep properties. Nevertheless, recently, the temperature problem of incremental block has been solved and computer programs were developed and many of them reported in the literature. In the greater part of them creep is considered very approximately [Majorana et al, 1990]. In several cases, standard codes of practice were used. However, due to the significant influence of creep on the stress values, especially in early age concrete [Santurjian and Kolarow, 1994] more accurate creep model is essential. In addition, continuous efforts should be made to establish reliably precise crack safety factor that, include the effect of temperature and time on its formation for a correct evaluation of the dam behavior.

The present investigation is continuation of authors' previous work [Noorzai et al, 2006]. The primary objectives of the present research work;

- a) To propose a viscoelastic model, which include the ageing and temperature effect on properties of concrete in its consideration.
- b) To apply the proposed model to a simple concrete block and an actual RCC dam to demonstrate the efficiency of the model.
- c) To determine the effect of temperature on the elastic properties and distribution of the stresses in the dam body during the construction phases.
- d) To examine the probability of cracking occurrence in the dam body due to temperature variation, dead load and creep.

## 2 Constitutive Relationships

### 2.1 Heat Diffusion

The general partial differential equation governing heat flow in a two-dimensional solid medium is expressed as [Incropera and DeWitt, 2002]:

$$\frac{\partial}{\partial x} \left( k_x \frac{\partial T}{\partial x} \right) + \frac{\partial}{\partial y} \left( k_y \frac{\partial T}{\partial y} \right) + \dot{Q} = \rho c \frac{\partial T}{\partial t} \quad (1)$$

where  $T$  is the solid temperature ( $^{\circ}\text{C}$ );  $k_x$ , and  $k_y$ , are the concrete conductivity coefficients in  $x$  and  $y$  directions respectively ( $\text{W/m } ^{\circ}\text{C}$ );  $\dot{Q}$  is the rate of the heat introduced per volume ( $\text{W/m}^3$ );  $\rho$  is the material density ( $\text{kg/m}^3$ ), and;  $c$  is the solid specific heat ( $\text{J/kg } ^{\circ}\text{C}$ ).

Two main types of boundary conditions are Dirichlet and Cauchy boundary, which can be written respectively as [Sergerlind, 1984]:

$$T = T_p \quad (2a)$$

$$T = T_p k_x \frac{\partial T}{\partial x} l_x + k_y \frac{\partial T}{\partial y} l_y + q + h(T_s - T_f) = 0 \quad (2b)$$

where  $T_p$  is the known values of the nodal temperatures on the boundaries;  $q$  is flowing heat from surface;  $h$  is the film coefficient;  $T_s$  is unknown temperatures at the boundary nodal points;  $T_f$  is the ambient temperature;  $l_x$ , and  $l_y$  are the direction cosines of the outward normal to the surface under consideration [Noorzaei et al, 2006].

### 2.2 Creep of Concrete

There are several creep models available in the literature. Most of the models are based on the assumption that creep varies linearly with stress [Westman, 1999], and they obey Boltzmann's principle of superposition. The most common models: the Bazant and Panula's (BP) Model [Bazant and Panula, 1982], ACI Model [ACI209, 1978], CEB-FIP model, Emborg model, Westman model [Westman, 1999], and the Exponential model [Bazant and Wu, 1974].

The exponential model has been attractive from the computation point of view, because it can avoid storing the whole stress history and made the implementation feasible comparing with other models.

The creep functions may be expressed with Dirichlet series [Bazant and Wu, 1974] as

$$J(t, \tau) = \sum_{\gamma=1}^M \frac{1}{\mu_{\gamma}(\tau)} [1 - e^{y_{\gamma}(\tau) - y_{\gamma}(t)}] \quad (3)$$

where  $J(t, \tau)$  is creep functions,  $\mu_\gamma(\tau)$  is function of one variable, called the reduced times,  $\tau$  is the loading age in days,  $y_\gamma$  is experimental function [Bazant and Wu, 1974].

Neglecting temperature effects, a specific form of the compliance function is often used [Zhu et al, 1976]

$$J(t, \tau) = C(t, \tau) + \frac{1}{E(t)} \quad (4)$$

where  $C(t, \tau)$  is creep compliance, it can be expressed as,

$$C(t, \tau) = \sum_{\gamma=1}^3 \varphi_\gamma(\tau) [1 - e^{-s_\gamma(t-\tau)}]$$

$$\varphi_1 = \alpha_1 + \beta_1 \tau^{-\delta_1}, \quad \varphi_2 = \alpha_2 + \beta_2 \tau^{-\delta_2}, \quad \varphi_3 = D e^{-s_3 \tau} \quad (5)$$

where  $\alpha_\gamma, \beta_\gamma, \delta_\gamma, D, S_\gamma$  are constants determined from the experimental data.

$E(t)$  is elastic modulus, and the model which developed by Conrad [Conrad et al, 2003], has been used in this study. This model expresses the variation of the elastic modulus of RCC material with time

$$E(t) = E_c e^{a\tau^b} \quad (6)$$

where  $E_c$  is the final elastic modulus,  $a$  and  $b$  are model parameters.

### 3 Temperature Effect

In the past, the material laws for hardening concrete were mainly based on the age of concrete. However, in reality, the temperature also influences the material's mechanical properties. If the temperatures increase, it will accelerate the initial elastic modulus of concrete, but the ultimate elastic modulus is not significantly affected [Bazant et al, 2004]. The creep rate also grows with higher temperature consequently creep strain is enlarged. It was shown that, a higher elastic modulus in the initial stage reduces the creep rate, but the creep increase always prevails [Du and Liu, 1994].

Bazant introduced the concept of the degree of hydration to include the temperature influence [Bazant et al, 2004]. Term equivalent age ( $\tau_e$ ), which represents the hydration period for which the same degree of hydration is reached at a current temperature as that one reached during the actual time ( $t$ ) at a reference temperature. The concrete age,  $\tau$ , will be replaced by equivalent age ( $\tau_e$ ) in the exponential model (Eq.5) [Wu and Luna, 2001].

$$\tau_e = \sum_0^\tau \beta_\tau(t) dt \quad (7a)$$

where  $\beta(t)$  is a function of current temperature and expressed as

$$\beta_{\tau}(t) = e^{\Pi_h(\frac{1}{T_r} + \frac{1}{T(t)})} \tag{7b}$$

where  $T(t)$  is a current temperature,  $T_r = 20^{\circ}C$ ,  $\Pi_h$  is function of hydration degree =2700 K. To consider the temperature effect on the creep compliance, a function  $y_{\gamma}(t)$  is introduced as

$$y_{\gamma}(t) = S_{\gamma} \sum_0^{\tau} \Psi_{\tau}(t) dt \tag{8a}$$

where  $\beta(t)$  is a function of current temperature and expressed as

$$\Psi_{\tau}(t) = e^{\Pi_{\alpha}(\frac{1}{T_r} + \frac{1}{T(t)})} \tag{8b}$$

where  $\Pi_{\alpha}$  is function of activation energy of creep =5000 K.

Introducing the ideas mentioned above into equations (5, 6) respectively

$$C(t, \tau) = \sum_{\gamma=1}^3 \varphi_{\gamma}(\tau_e) \left[ 1 - e^{-s_{\gamma}(t-\tau)} \right] \tag{9}$$

Using the introduced term of equivalent age ( $\tau_e$ ), which represents the hydration period, the concrete age,  $\tau$ , will be replaced with this equivalent age ( $\tau_e$ ) in the above elastic modulus (Eq.(6)). So modified model includes the aging and temperature effects on the elastic modulus.

$$E(t) = E_c e^{a\tau_e^b} \tag{10}$$

#### 4 Mathematical Model of Creep

Du and Liu, 1994, introduced the numerical procedure for creep strain in mass concrete structure with temperature effects by modifying the exponential algorithm for concrete developed by Bazant.

The total strain column vector within the  $n$ th interval may be generalized as

$$\{\Delta \epsilon_n\} = \{\Delta \epsilon_n^e\} + \{\Delta \epsilon_n^c\} + \{\Delta \epsilon_n^T\} \tag{11}$$

where  $\{\Delta \epsilon_n^e\}$ ,  $\{\Delta \epsilon_n^c\}$ ,  $\{\Delta \epsilon_n^T\}$  refer to elastic, creep, temperature strain increment column vectors, respectively.

From  $t_0$  to  $t$ , the creep strain may be expressed as [Du and Liu, 1994]

$$\{\epsilon^c(t)\} = [Q] \{\sigma_0\} C(t, t_0) + [Q] \sum_{t_0}^t C(t, \tau) \left\{ \frac{\partial \sigma}{\partial \tau} \right\} d\tau \tag{12}$$

where  $\sigma$ ,  $\sigma_0$  are the transient and initial stresses respectively.  $[Q]$  matrix can be expressed as

$$[Q] = \begin{bmatrix} 1 & -\nu & 0 \\ -\nu & 1 & 0 \\ 0 & 0 & 2(1+\nu) \end{bmatrix} \tag{13}$$

where  $\nu$  is the Poisson's ratio

The total time travel  $[t_0, t]$  is subdivided into  $N$  steps, for the step  $[t_{i-1}, t_i]$  and substituting equations 5 and 6 into equation 12 and integrating the equation. The resulting equation;

$$\{\epsilon^c(t)\} = [Q] \sum_{\gamma=1}^3 \left\{ \sigma_0 \phi_{\gamma}(t, 0) [1 - e^{-y_s(t)}] + \sum_{i=1}^N \frac{\Delta\sigma_i}{\Delta\tau_i} \sum_{\tau_{i-1}}^{t_i} \phi_{\gamma}(\tau_e) [1 - e^{-(y_s(t)-y_s(\tau))}] d\tau \right\} \tag{14}$$

Performing the integral mean value theorem, Eq.14 can be rewritten as [Du and Liu, 1994]

$$\{\epsilon^c(t)\} = [Q] \sum_{\gamma=1}^3 \left[ \sigma_0 \phi_{\gamma 0} (1 - e^{-y_s(t)}) + \sum_{i=1}^N \Delta\sigma_i \phi_{\gamma i} [1 - f_{\gamma i} e^{-y_s(t)}] d\tau \right] \tag{15a}$$

where

$$f_{\gamma n} = \frac{1}{\Delta\tau_n} \sum_{\tau_{n-1}}^{t_n} e^{y_s(\tau)} \tag{15b}$$

The creep strain increment column vector within step  $[t_{n-1}, t_n]$  may be generalized as

$$\{\Delta\epsilon^c\} = [Q] \sum_{\gamma=1}^3 [(1 - e^{-s_{\gamma}\Psi_{\tau_n}\Delta\tau_n}) \{\omega_{\gamma n}\} + \{\Delta\sigma_n\} \phi_{\gamma n} h_{\gamma n}] = \{\eta_n\} + q_n [Q] \{\Delta\sigma_n\} \tag{16a}$$

where;

$$\{\eta_n\} = \sum_{\gamma=1}^3 [(1 - e^{-s_{\gamma}\Psi_{\tau_n}\Delta\tau_n}) \{\omega_{\gamma n}\}] \tag{16b}$$

$$\{\omega_{\gamma n}\} = \{\omega_{\gamma n-1}\} e^{s_{\gamma}\Psi_{\tau_{n-1}}\Delta\tau_{n-1}} + [Q] \{\Delta\sigma_n\} \phi_{\gamma n-1} f_{\gamma n-1} e^{-Y_{n-1}} \tag{16c}$$

$$q_n = \sum_{\gamma=1}^3 \phi_{\gamma n} h_{\gamma n} \tag{16d}$$

$$h_{\gamma n} = 1 - f_{\gamma n} e^{-Y_n} \tag{16e}$$

$$Y_n = S_n \sum_{j=1}^n \Psi_{Tj} \Delta T_j \tag{16f}$$

from Eqs.(11) and (16) the increment in the stresses at  $n^{th}$  time interval.

$$\{\Delta\sigma_n\} = [D'_n] (\{\Delta\varepsilon_n\} - \{\eta_n\} - \{\Delta\varepsilon_n^T\}) \tag{17a}$$

$$[D'_n] = \frac{[D_n]}{(1 + q_n E_n)} \tag{17b}$$

where  $[D_n]$  is the elastic matrix for plane strain problem at the  $n^{th}$  time interval, which has been calculated based on the model in Eq.10. Consequently,  $[D_n]$  can be redefined as elastic matrix for RCC material which includes the aging and temperature effect.

By the equilibrium equation of the finite element method, we obtain

$$[K_n] \{\Delta\delta_n\} = \{\Delta P_n^c\} + \{\Delta P_n^T\} + \{F\} \tag{18}$$

where  $[K_n]$  is the global stiffness matrix,  $\{\Delta\delta_n\}$  is the column matrix of nodal displacement,  $\{\Delta P_n^c\}$  is equivalent load column matrix of nodal creep,  $\{\Delta P_n^T\}$  is equivalent load column matrix of nodal thermal force,  $\{F\}$  is external force.

The column matrix of nodal stresses at the moment of  $n^{th}$  step is

$$\{\sigma_n\} = \{\sigma_{n-1}\} + \{\Delta\sigma_n\} \tag{19}$$

### 5 Cracking Criteria

In the previous work of the authors the crack index has been used to evaluate the safety of the dam against the crack, where the crack index presented the ratio of the tensile strength to maximum principle stress which was approximate cracking criteria. The assessment of the crack occurrence is performed by using the cracking criterion coefficient suggested by Kupfer [Kupfer and Gerstle, 1973], which is a function of the principal stresses. The safety coefficient against cracking criterion is defined by the following formula:

$$C_f = \frac{\sigma_{ult}(t)}{\sigma_1(t)} \tag{20}$$

where  $\sigma_1(t)$  and  $\sigma_{1(ult)}$  are the RCC maximum and allowable principle stresses respectively.  $\sigma_{1(ult)}$  depends on the types of the maximum and minimum principle stresses.

(i) For tension-tension, Kupfer and Gerstle suggested a constant tensile strength equal the uniaxial tensile strength of concrete.

$$\sigma_{1(ult)}(t) = f_t(t) \quad (21a)$$

(ii) For tension-compression, Kupfer and Gerstle suggested a straight line reduction in tensile strength.

$$\sigma_{1(ult)}(t) = f_t(t) \left(1 + 0.8 \frac{\sigma_2(t)}{f_c(t)}\right) \quad (21b)$$

where  $f_t(t)$  is the RCC tensile strength at the time  $t$ .  $f_c(t)$  is the compressive stress of concrete.

If safety coefficient of crack is greater than one, the element will be considered safe against crack. But if the coefficient is less than one, crack will develop in the dam body.

## 6 Computational algorithm of creep and temperature effect

The computational procedures followed in this study to account for creep and temperature effects are summarized as follows:

1. Using procedure in the section 2 the temperature field  $T(t)$  is computed.
2. Substituting  $T$  into Eqs (7), (8),  $\beta_T$  and  $\Psi_T$  will be evaluated using;

$$\beta_\tau(t) = e^{\Pi_h(\frac{1}{T_r} + \frac{1}{T(t)})}, \quad \Psi_\tau(t) = e^{\Pi_\alpha(\frac{1}{T_r} + \frac{1}{T(t)})}$$

3. Determine the equivalent age and elastic modulus for the  $n^{th}$  interval time
4. Generate the constants of Eq. (16)
5. Calculate  $q_n$ ,  $\{\eta_n\}$
6. Calculate the equivalent nodal loads include, temperature, creep, external.
7. Solve Eq. (18) to obtain the column matrix of nodal displacement increment, and based on that calculate the column matrix of stress increment at  $n$ th time interval.

8. Calculate the total stress at nth time using Eq.(19).
9. Repeat step (1) to (8) until the construction of the stage is completed.

Fig.1 illustrates the code flow chart based on the above computational steps.

## 7 Computational Procedures for Safety Evaluation Against Cracking

The crack analysis is determined by calculating the safety coefficient against cracking criterion  $C_f$ , which is given in Eq. 20. The variation in the compressive strength with time is calculated according to ACI, which relates the elastic modulus to the compressive strength as

$$E(t) = 4750\sqrt{f_c(t)} \quad (22)$$

where  $E_c(t)$  is the elastic modulus, that is determined based on the procedures in section 3 of this article, which is time and temperature dependent.

In order to determine the tensile strength, the splitting tensile strength of RCC material is evaluated using the model that developed by Zdiri [Zdiri et al, 2008] Eq.(23). The latter (splitting tensile strength) will be changed to direct tensile strength using Eq.(24) which is given by Malkawi [Malkawi and Mutasher, 2003].

$$f_{sp} = 0.214 f_c^{0.69} \quad (23)$$

$$f_t = 0.722 f_{sp}^{0.9} \quad (24)$$

By combining the above Eqs. (23), and (24) the direct tensile strength of RCC materials could be expressed as:

$$f_t = 0.18 f_c^{0.621} \quad (25)$$

Finally, the allowable principle stress will be determined using Eq.(21) based on that the crack safety factor is generated by Eq.(20). Fig.2 illustrates the above computational steps.

## 8 Development of Finite Element Code

The two dimensional finite element software developed by Noorzai et al. (2006) have been significantly modified [Abdulrazeg, 2010]. The followings are the features of development computer code:

- a) Thermal analysis.

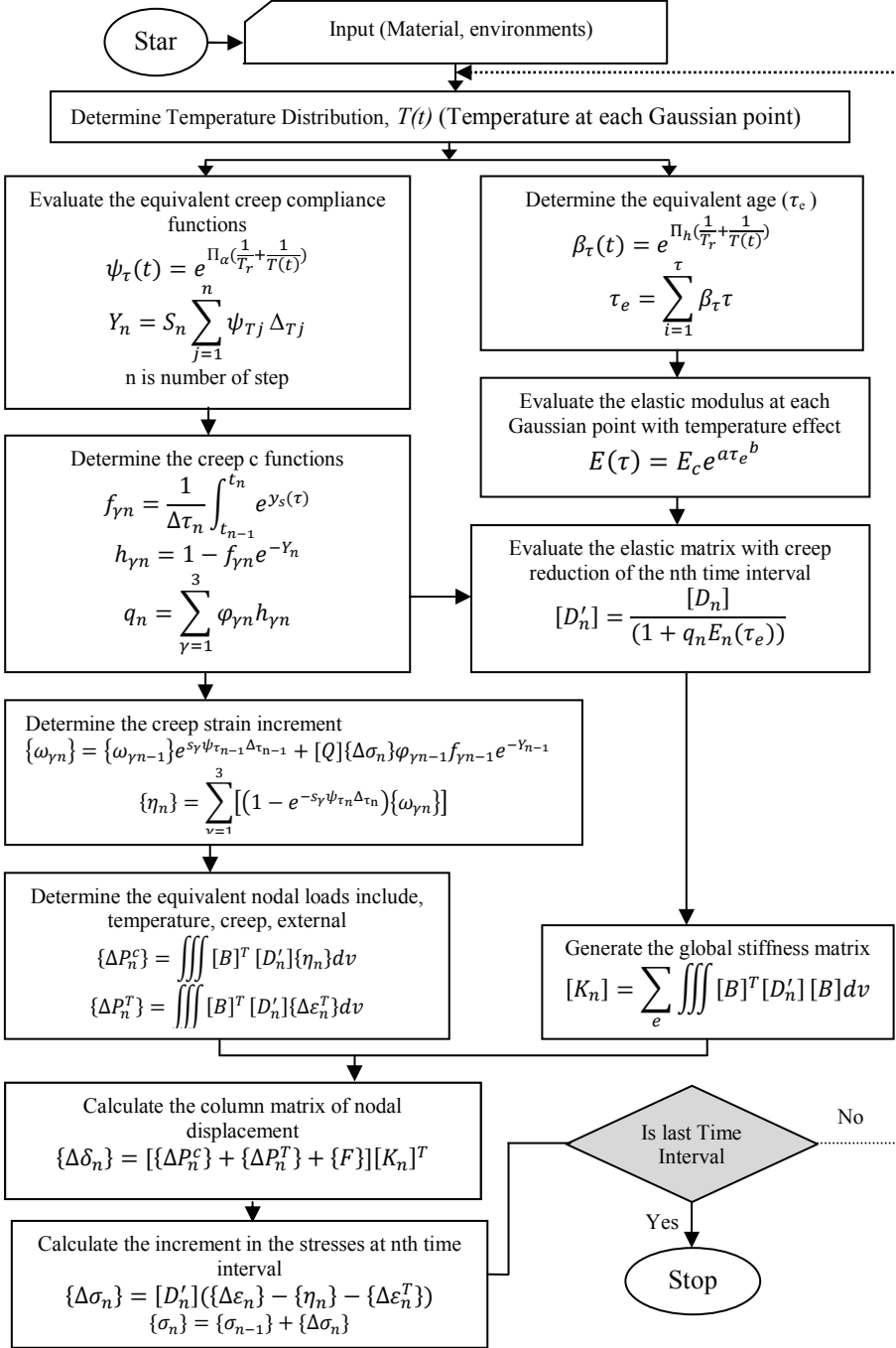


Figure 1: Program flow chart for computational procedures of creep and temperature effect

- b) Thermal and structural analysis
- c) Thermal and structural analysis including creep
- d) Crack prediction.

The structure will be divided into stages according to construction schedule; each stage will be divided into several times. The thermal analysis will be preformed first, if only the temperature field analysis is desired, then the program moves to the next time step. If the coupled analysis is also desired, then the computations for stress analysis are activated, and in case the creep is taken into consideration, the computational procedures in the section 5 will be preformed. The general procedures followed in the stress analysis are presented in Fig .3[Abdulrazeg, 2010].

The developed finite element program is written in Fortran language and can work under power station environment. The developed finite element program has the capability to perform;

1. Thermal analysis
2. Structural analysis with or without creep effect
3. Thermal and structural analysis with or without creep

In structural or combined analysis the creep effect could be include. For this purpose a predefined index such *ICREEP* has been assigned so that when *ICREEP=0* is without creep, *ICREEP=1* is with creep.

## 9 Verification of the Proposed Model

The validity of the proposed methodology has been established by analyzing a concrete block and comparing the results obtained against those available in the literature. The block geometry is shown in Fig.4. The material properties are summarized in Table 1. The upper surface of the block is exposed to the air and the ambient temperature is 10 °C. The creep constants for concrete material were obtained from report done by Zahang and summarized on Table 2 [Zahang, 1995].

Fig.5 shows the temperature and the variation of the elastic modulus at the central point of the concrete block. The temperature increase due to the heat produced by hydration, then reaches a maximum point about 4 days after casting. Then the block starts to cool down due to the interaction with ambient temperature. The plot shows also the variation of the elastic modulus with time at the central point. It is obvious form the plot, due to high temperature of hydration at the initial time the elastic modulus will be accelerated. But the block starts to cool down and its

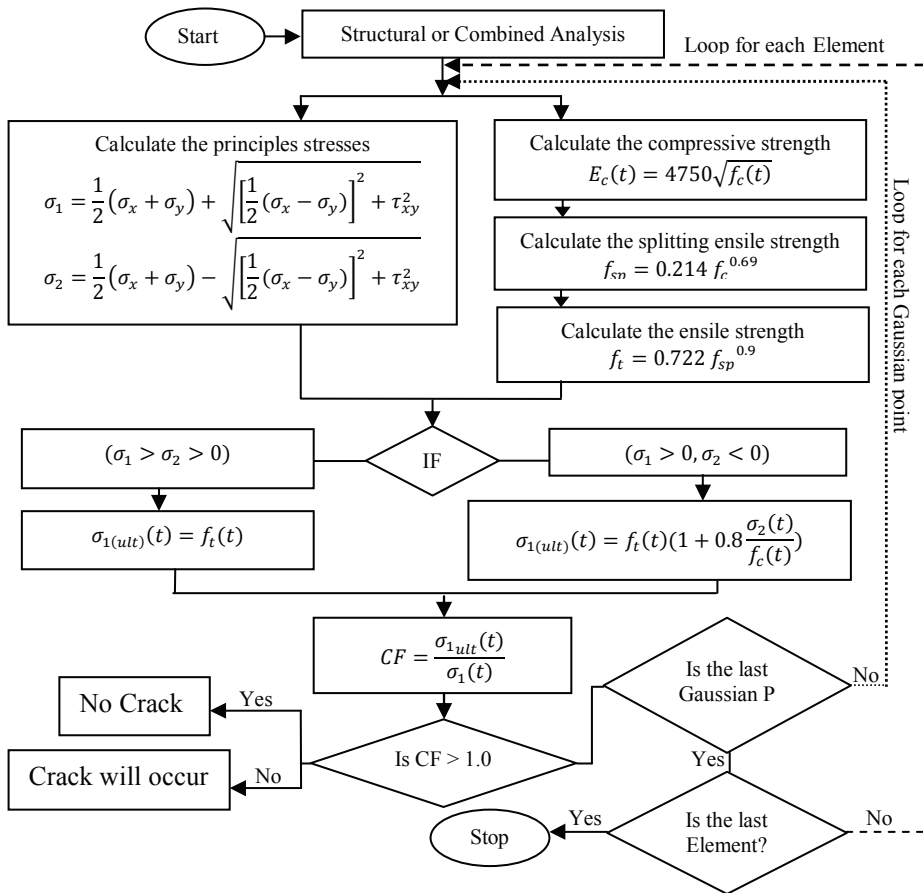


Figure 2: Program flow chart for computational procedures of crack coefficient

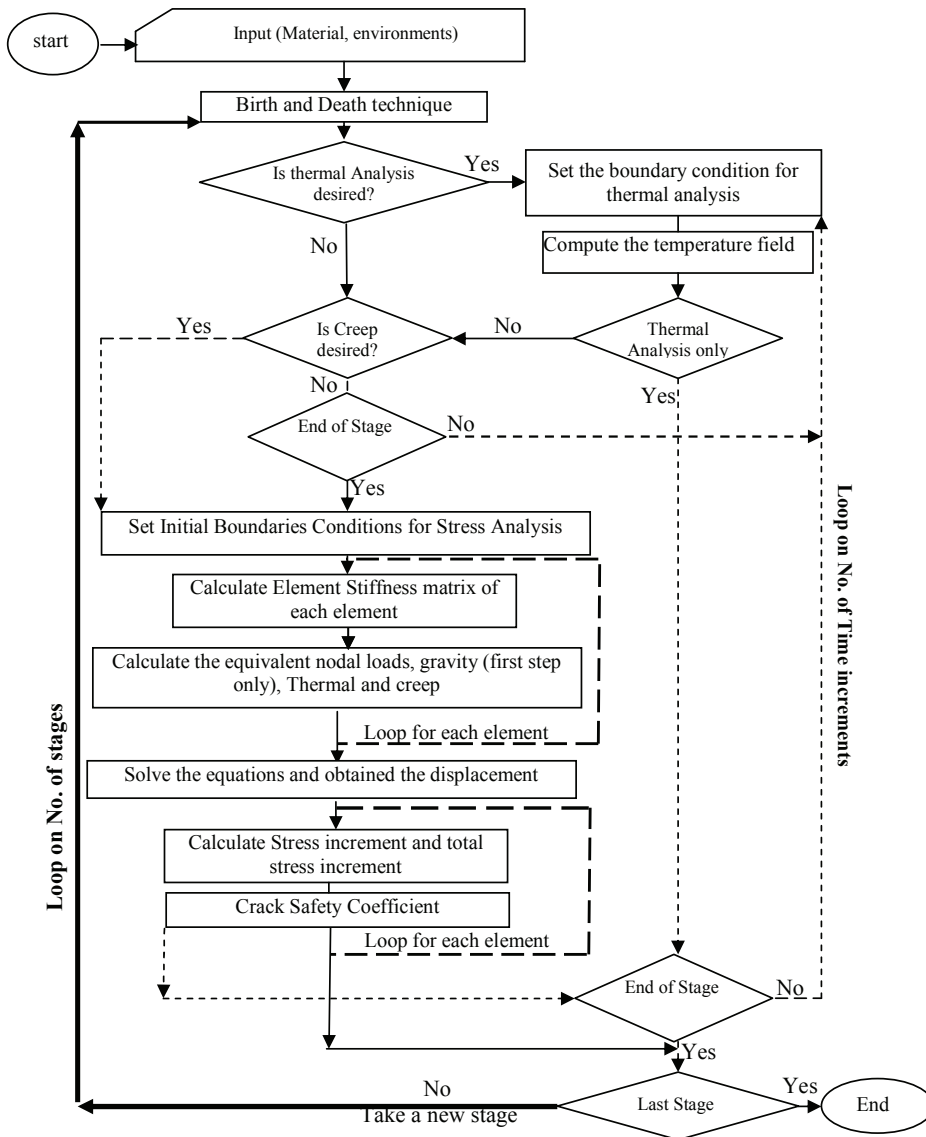


Figure 3: Program flow chart (with temperature and creep modification)

Table 1: Thermal and structural properties of concrete block [Noorzaei et al. 2009]

Material	RCC	Rock
Heat conduction coeff. $K$ (W/m °C)	2.7	2.97
Heat convection coeff. $h$ (W/m <sup>2</sup> °C)	8.0	8.0
Specific heat $c$ (J/kg °C)	1150	800
Density $\rho$ (kg/ m <sup>3</sup> )	2325	2650
Elasticity modulus $E$ (MPa)	18200	24000
Poisson ratio $\nu$	0.2	0.2

Table 2: Creep Constants[Zahang, 1995]

	$\alpha$	$\beta$	$\delta$	D
1	0.35494	0.48368	0.35361	.....
2	3.7335	-0.186	0.012486	.....
3	- 2.5644	0.13786	0.032642	0.83509

temperature drop below 20 °C the elastic modulus will be decelerated due to lower temperature.

Fig.6. shows the thermal stress ( $\sigma_x$ ) variation with age at the center of the block for different cases (case I without temperature effect, case II with temperature effect). The plot was made to study the effect of temperature on the thermal stress development. It's evident from the plot that, there is marginal different between two cases. In the case. II the thermal stress has been decreased at the initial stage and was increased later on the final stage, the similar response has reported by Du [Du and Liu, 1994]

Fig.7 shows the stress development with age at the central of the block without including thermal stress development (gravity load only). There is an increase in the compression stress due to temperature and creep effect. Similar response was reported by Yuan [Yuan and Wan, 2002]. A higher elastic modulus in the initial stage reduces the creep rate, but the creep increase always prevails. Fig.8 shows the cumulative increment of stresses ( $\sum \Delta \sigma_y$ ) at nth time for different ages of loading. Age of loading play a significant role on the creep value, which is manifested by a significant decrease of creep with the age at loading.

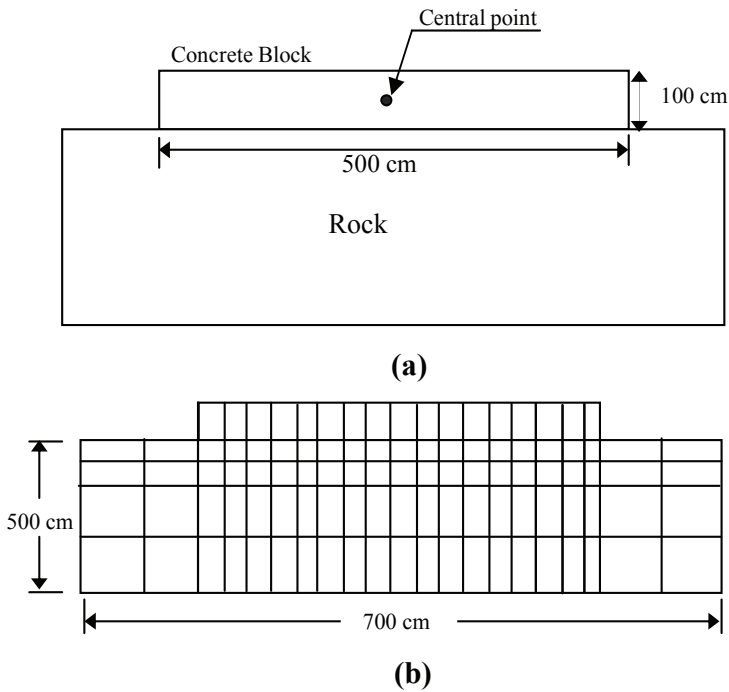


Figure 4: (a): Concrete Block; (b): Discretization of the Concrete Block

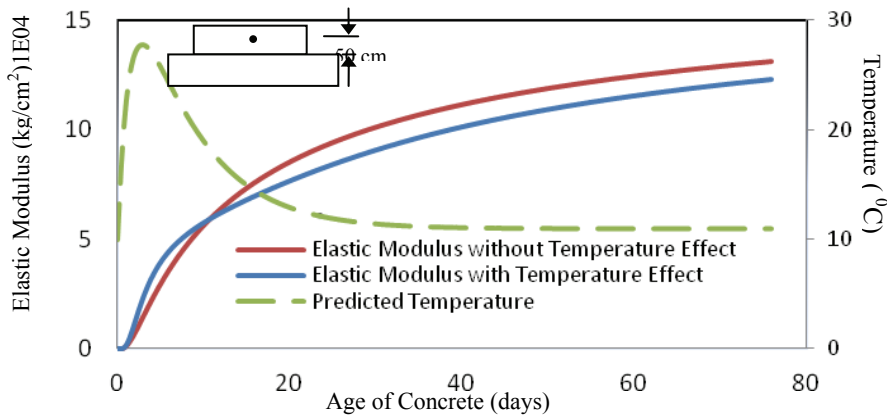


Figure 5: Temperature and elastic modulus variation at the central point

### 10 Analysis of Actual RCC Dam

The Sg. Kinta dam located approximately 12 km north east of Ipoh in Malaysia, which forms part of the Greater Ipoh Water Supply Scheme phase II was completed

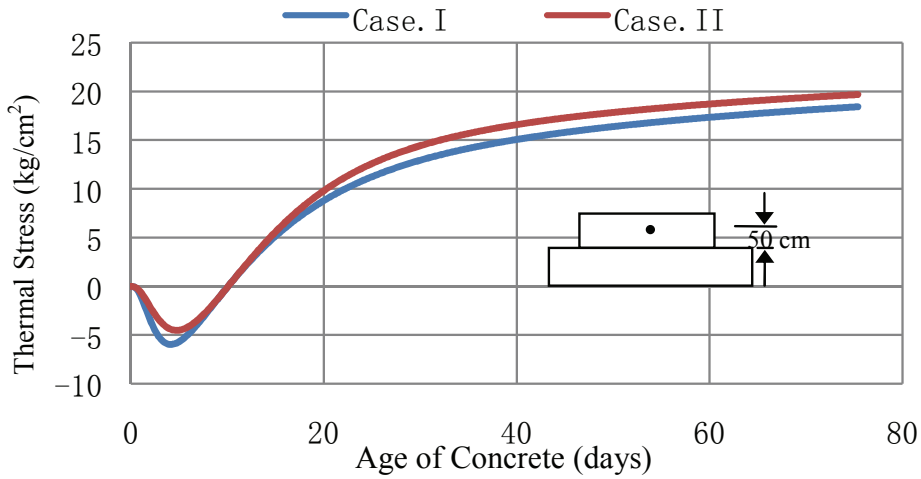


Figure 6: Thermal stress at the central point of the block

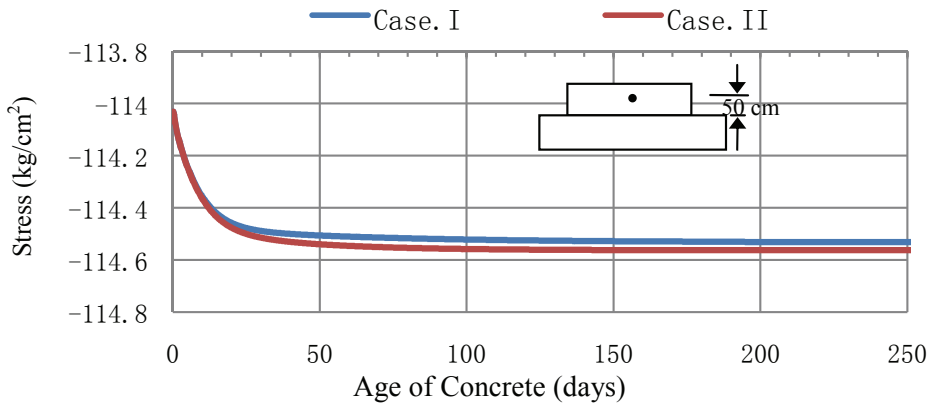


Figure 7: Stress Development at central point of the block with age

in 2006. The maximum height of the dam is 78 m and the crest length is 700 m [SUNGAI Kinta dam (2002)]. The progress of the dam construction with respect to time, materials properties, and the site recorded hourly environmental temperatures were given in the previous work of author [Noorzaei et al. 2009]. They will not be reproduced in the present work. The creep experimental data which reported in the literature [Zhang, 1995] for RCC and CVC materials has been used in present study, these data tabulated in the Table 3.

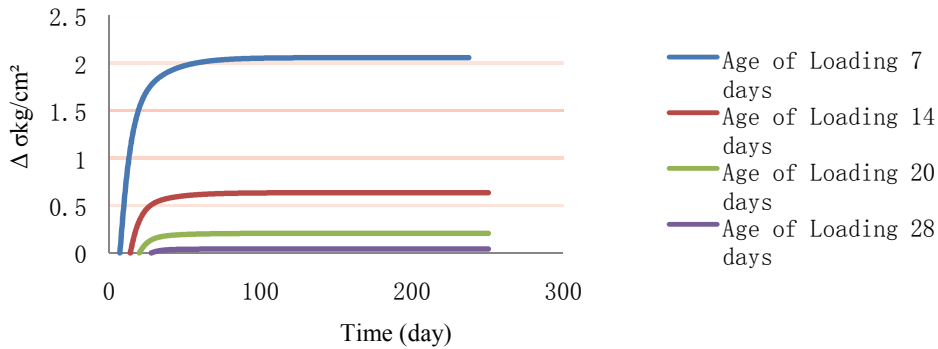


Figure 8: Cumulative increment of stresses ( $\sum \Delta\sigma_y$ ) with different age of loading at central point

Table 3: Creep data for RCC and CVC materials[Zhang, 1995]

Material	$\alpha$		$\beta$	$\delta$	D
CVC	1	0.35494	0.48368	0.35361	.....
	2	3.7335	-0.186	0.012486	.....
	3	-2.5644	0.13786	0.032642	0.83509
RCC	1	0.058864	0.38362	1.356	.....
	2	7.4729	-11.115	0.08919	.....
	3	-5.2079	7.9619	0.078675	4.2808

### 10.1 Finite Element Modeling

The 2D finite element model of the deepest block is shown in Fig.9. Eight noded isoparametric elements are used in the analysis. The mesh of the dam body is generated in such a way to simulate the construction phase.

## 11 Result and Discussion

### 11.1 Temperature Distribution During Construction

The contours of the temperature distribution in the dam body for stages 10, 18, and the final stage are presented in the Fig.10.

Fig.10(a) illustrates the contours of the temperature distributions within the dam's body after completion of the 10th stage. The maximum temperature observed was 44 °C, it was formed at the bottom of the dam. This is attributed to the use of

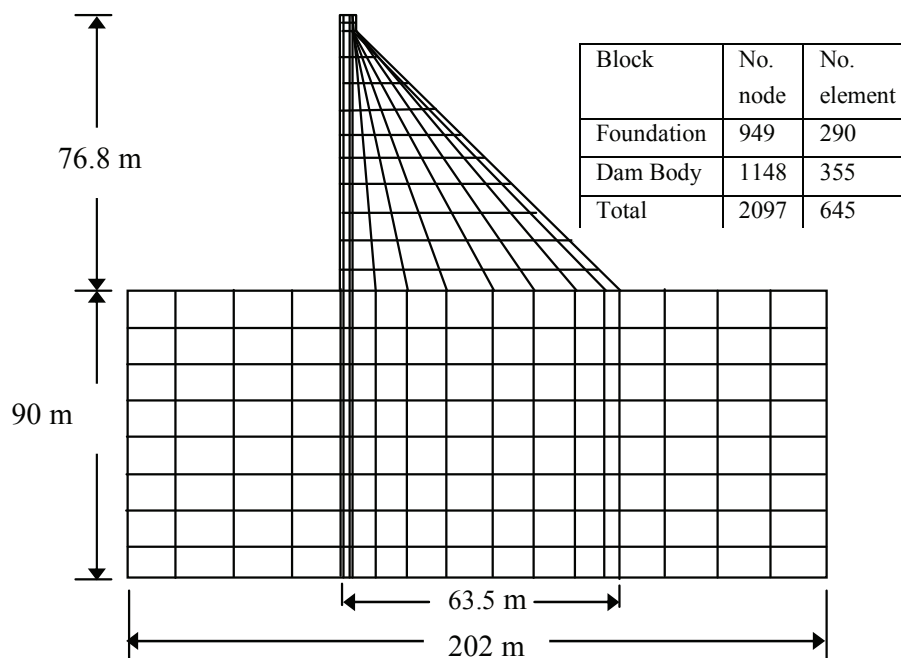


Figure 9: 2-D Finite Element mesh

higher RCC placing temperatures combined with the higher insulating property of this region due its massive volume compared with the other locations.

Fig.10(b) shows the isothermal contours obtained immediately after the end of construction of the 18<sup>th</sup> stage. The maximum predicted temperatures was formed at the top of the dam that because, the hydration process is still high in this area comparing with other dam body. The temperature at the center of the dam was 42 °C and it decreased to reach the air temperature at the boundary condition.

Isothermal contour plot at the end of the dam construction is shown in Fig.10-c. The plot shows that, the higher temperature zone is at the center of the dam body with maximum predicted temperature of 42 °C, which gradually decreased to reach approximately the air temperature at the boundaries.

Generally, from the isothermal contour of different stages, it can be conclude that, there are three different zones, which are outer zone, middle zone, and central zone. The maximum temperature is formed at the central zone due to the width effect, where the cooling takes place slowly. On the other hand, minimum temperature has been observed at the outer zone, which almost reaches the air temperature due

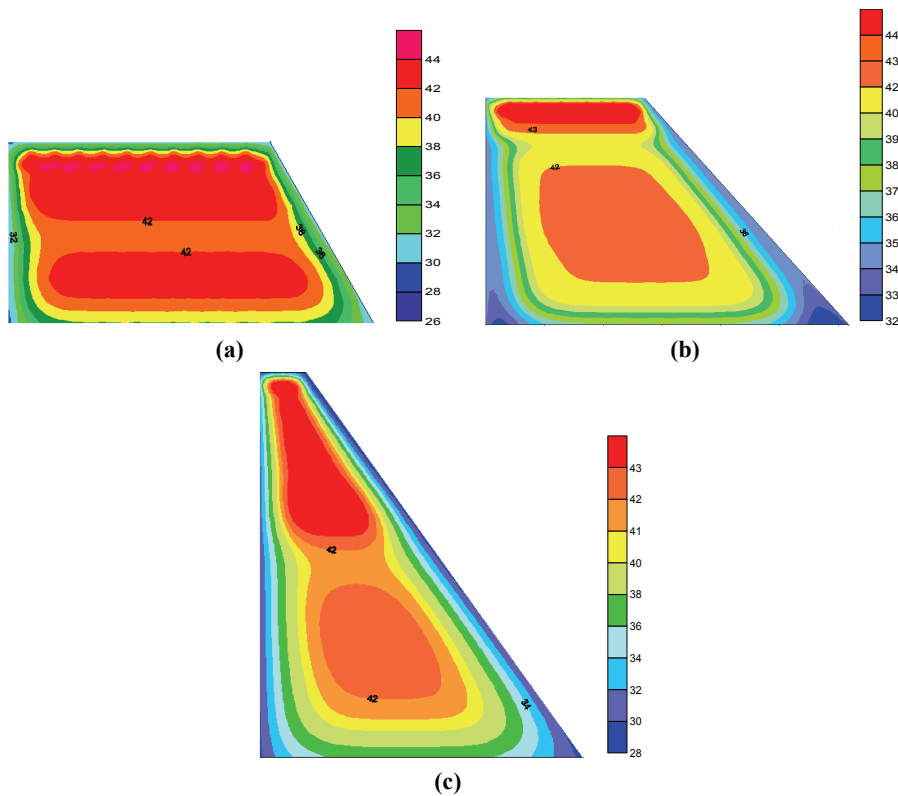


Figure 10: (a): Temperature Distribution for stage No. 10; (b): Temperature Distribution for stage No. 18; (c): Temperature distribution after completing the dam construction

to the environmental active. The middle zone is representing the gradually change of temperature from the maximum grade at the boundary of central zone to the minimum grade at the boundary of outer zone.

After the temperature field was computed, the methodology proposed in the Section 3 of this research has been activated to determine the variation of the elastic modulus with time considering the temperature effect.

In order to illustrate the effect of the temperature on the variation of the elastic modulus, Fig.11 has been plotted to show the temperature at the particular point (a). The temperature increases due to the heat produced by hydration, then reaches a maximum point at about 5 days after casting. It is obvious from the plot there is a significant difference between the two curves of the elastic modulus during the initial stage due to the high temperature of hydration. If the temperature effect was

considered the elastic modulus is increased by 44% and 24% in the first two and four weeks respectively. The ultimate elastic modulus is not significantly affected, where there is increase in the elastic modulus by 4% after 300 days from casting if the temperature was considered.

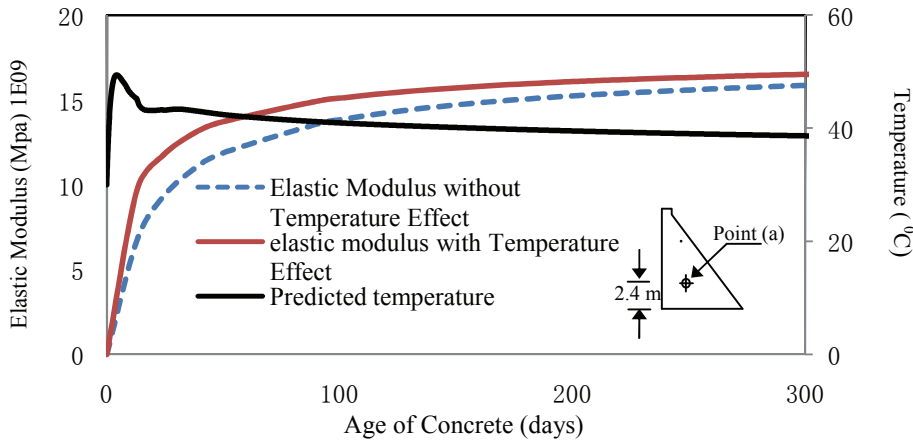


Figure 11: Temperature and the variation of the elastic modulus at the central point

## 11.2 Stress Simulation during Construction

A viscoelastic model, including ageing and temperature effects was adopted for the stress analysis. The same time interval for the heat transfer problem and the stress analysis was used in this study. Initially the thermal analysis is performed with time step. The degree of equivalent hydration period is evaluated. Based on this degree the elastic modulus and creep are calculated.

In order to illustrate the effect of temperature on the development of stresses within the dam body maximum principle stresses have been drawn for different axes of the dam body as indicated in Fig.12.

Fig.13 shows the variation of maximum principle stress along axis of a-a within the dam after completion of second stage within age of two weeks. It's clear that, the stress has been increased. When the temperature effects are considered, the maximum principle stresses increased from 0.87 MPa to 1.22 MPa by 40% in the initial stage. This is because the temperature at the initial stage is high due to hydration the elastic modulus is high also which increased the stress during this stage. However, the ultimate elastic modulus is not significantly affected by the temperature

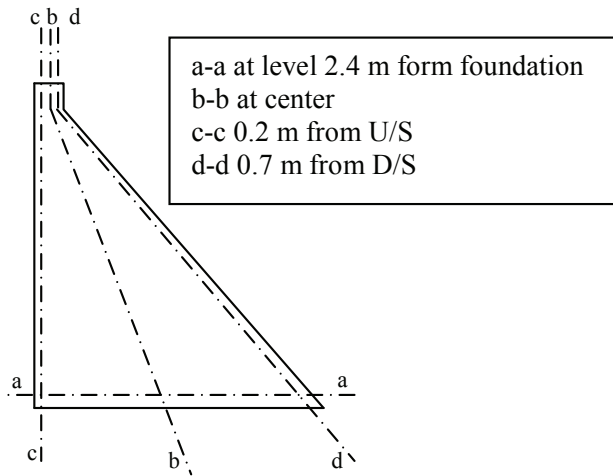


Figure 12: Diagram of the Dam

and higher elastic modulus reduces the creep rate. Therefore, the stresses will not be much effected comparing with initial stage.

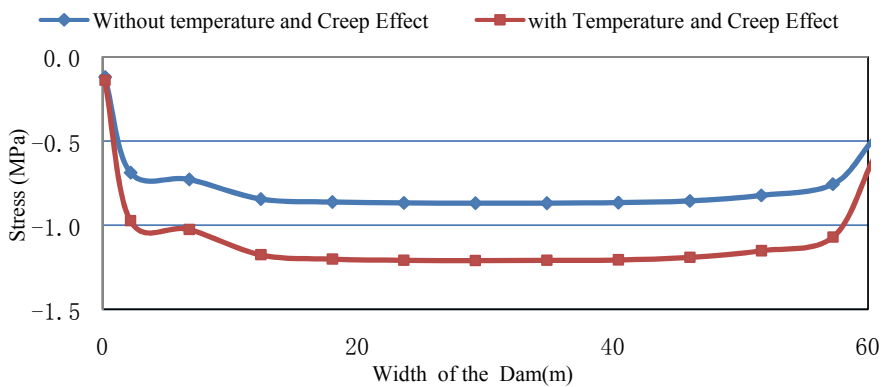


Figure 13: variation of Maximum principle Stress along axis of a-a

Fig.14. Shows the variation of maximum principle stress along different axis's (b-b, c-c, and d-d) at the end of construction, these plots are made for the three sections namely b-b, c-c, and d-d. Similar response to the axis a-a has been shown by other axis. Since, each layer has different age, consequently different mechanical properties, thermal and creep properties. Therefore, the effect of temperature and

creep also different from layer to layer. Generally there is increasing in the stresses if the temperature effects and creep were considered.

Fig.15 shows the principal stress distribution  $\sigma_1$  (MPa) for different construction stages, It is clearly observed from these plots, the presence of high tensile stresses at the dam bottom and the boundaries. While compressive stresses contours are concentrated the dam body with high values at the lower levels of the upstream face. Generally, it is observed that most of the dam body under compressive stresses and it increased with construction stages.

Fig.16 shows the distribution of the minimum principal stress  $\sigma_3$  (MPa) for different construction stages. High compressive stress zones concentric at the bottom of the dam which gradually reduces toward the boundaries. In addition small regions of high compressive stresses have been observed lower points of upstream and downstream.

### ***11.3 Cracking Criteria and Safety Evaluation***

After the stress analysis is preformed, the crack safety factor will be calculated based on the Eq.(20) for each Gaussian point. Hence, all the properties of the materials are time and temperature dependent, especially elastic and strength properties, the variation of the crack factor with time and temperature are determined. Thus, this factor will be more realistic to represent the crack occurrence.

The crack safety factor with time for two levels (2.4 m and 11.4 m) across the dam's width has been shown in the Figs.17, 18. It is clear from the plots that the dam is safe against cracking for points P1 and P2, even though the factor at the elevation of 11.4 m drops below the allowable limit (1.0) for P1, but this drop was in the initial time where the concrete can be considered to be young concrete.

In case of P3, which is located at downstream side. It is obvious from the Fig.14 the tensile stress which developed at the downstream is higher than those developed at the upstream, which leads to this drop in the crack safety factor in this zone, it can be concluded that special attention should be paid to this side in design. It can conclude that, the upstream and the downstream regions at this level (toe and hill) are the most probable crack regions where the crack index values are dropped below the limit value.

## **12 Conclusions**

The temperature effect on the elastic and creep properties of RCC dams has been ignored by the most of the earlier researcher. In addition, the creep phenomena in the structural response of RCC dams have not been addressed sufficiently, partly because of the complexity of the problem and the extensive computational effort

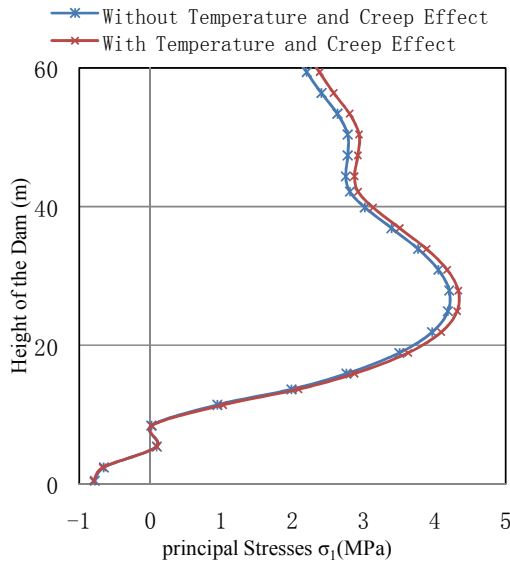
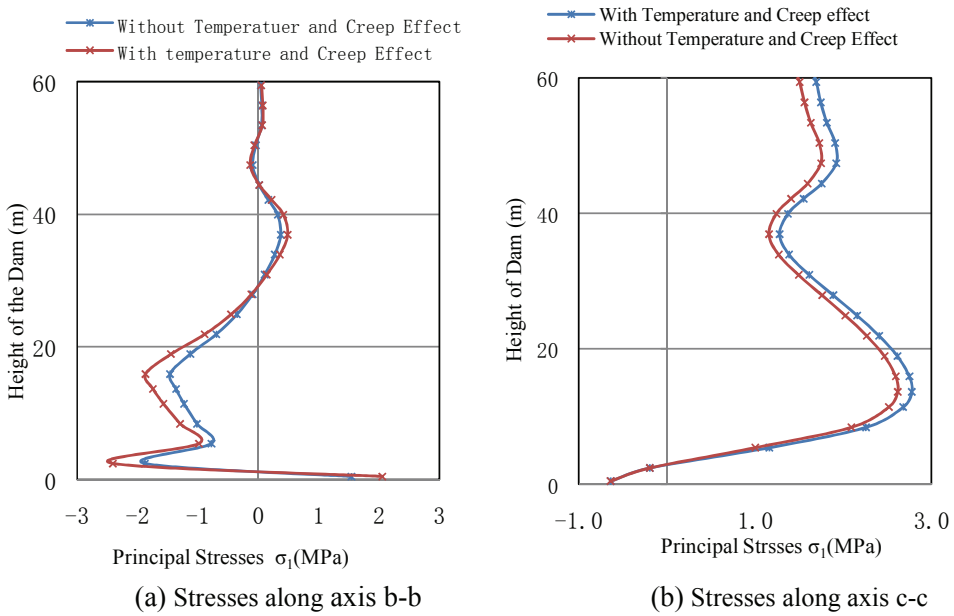


Figure 14: Variation of the maximum principle stress with the dam's height

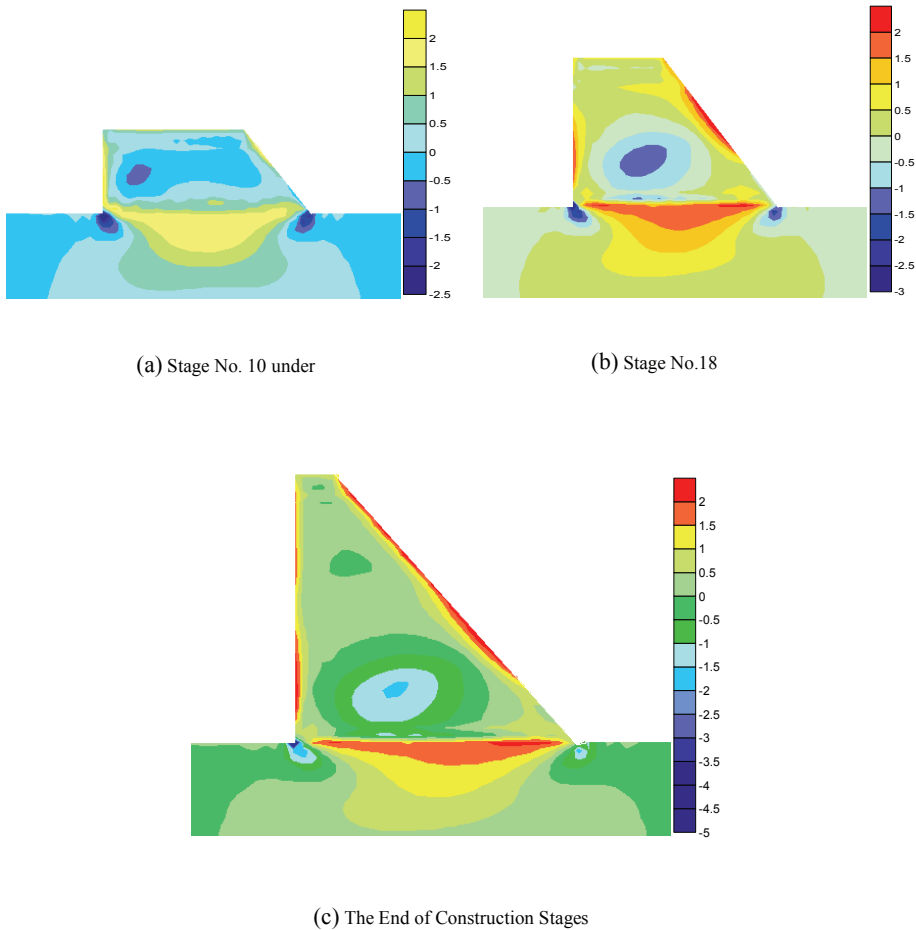


Figure 15: Maximum Principal Stresses  $\sigma_1$  (MPa)

required carrying out such phenomena. Hence, the proposed viscoelastic model can be effectively used for analysis of RCC dams by considering the ageing effects and thermal dependent properties for the RCC materials.

Based on the present study, the following points can be drawn;

1. A viscoelastic model, that include ageing and temperature effects on properties of RCC materials was developed.
2. The Conrad's model which expresses the variation of the elastic modulus of RCC material with time, has been further modified to account for tempera-

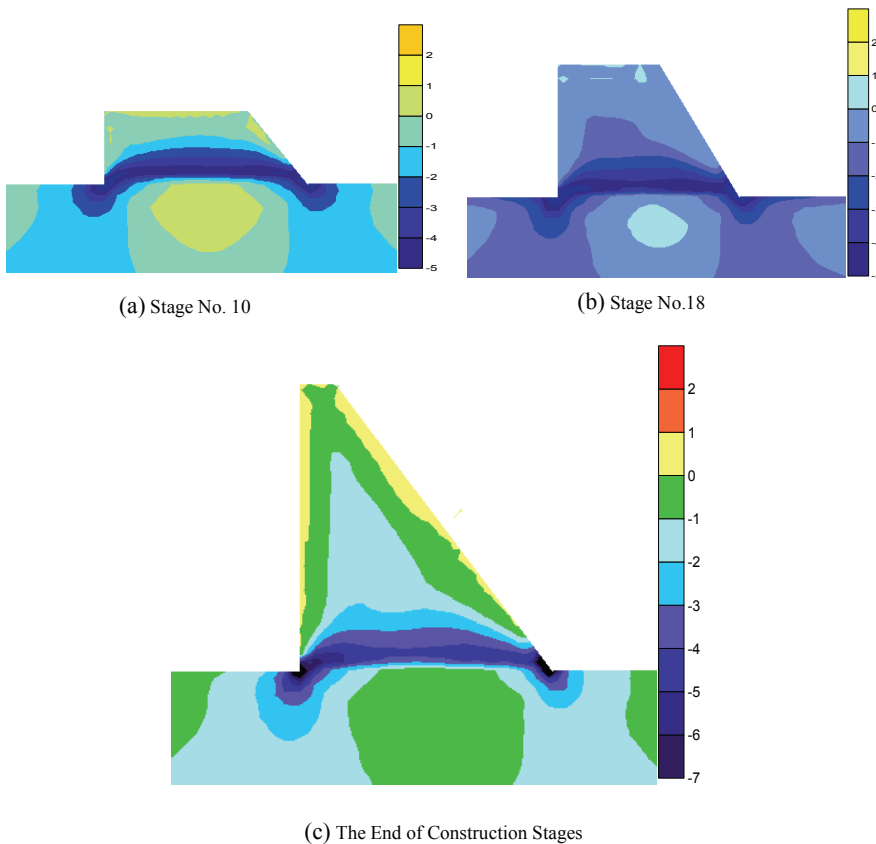


Figure 16: Minimum Principal Stresses  $\sigma_3$  (MPa)

ture effect.

3. The result has shown that, If the temperature effects are considered, the maximum principle stresses increased by 40% in the initial stage. This is because the temperature at the initial stage is high due to hydration the elastic modulus is high also which increased the stress during this stage.
4. The crack index variation can give a good indication of the probability of cracking with time.
5. The exposed dam boundaries possess the same air temperature at the end of each stage of analysis.
6. The tensile stress which developed at the downstream is higher than those

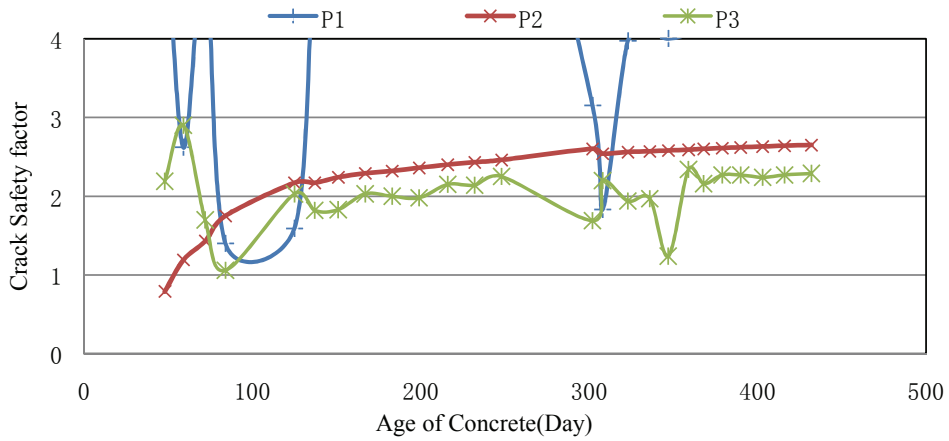


Figure 17: Crack Safety factor variation at level of 2.4 m

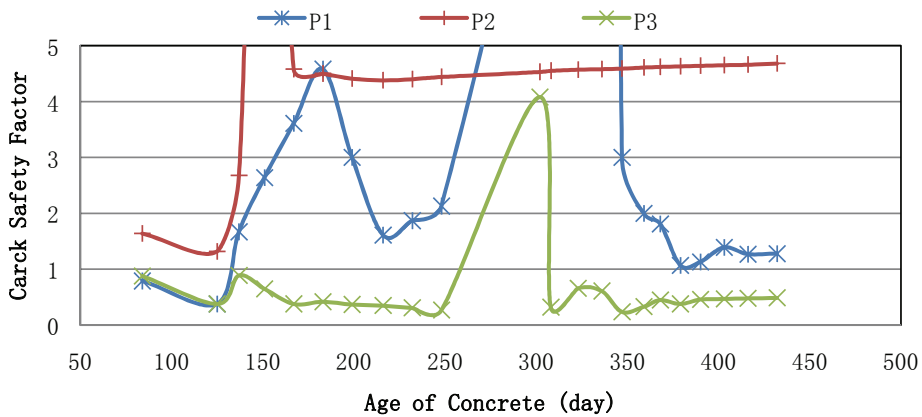


Figure 18: Crack Safety factor variation at level of 11.4 m

which developed at the upstream, which leads to this drop in the crack safety factor in this zone, it can be concluded that special attention should be paid to this side in design.

7. Remarkably high tensile stress was observed at the downstream side. Hence special attention should be paid to this side in design.

**Acknowledgement:** The authors are grateful for Lembaga Air Perak and Angkasa-

GHD SDN Bhd in Malaysia for helping in giving some data used in the preparation of this paper. The authors would also like to recognize the general peoples committee for higher education Libya for the financial support provided to Mr. A. A. Abdularzeg during his PhD program at Universiti Putra Malaysia.

## References

- Abdulrazeg, A.A.** (2010) Analysis of Roller Compacted Concrete Dam, *PhD thesis*, Universiti Putra Malaysia, Malaysia, in progress.
- Araujo ,J. M.; Awruch, A. M.** (1998): Cracking Safety Evaluation on Gravity Concrete Dams during the Construction Phase, *Computers and Structures*, Vol. 66, No. 1, pp. 93-104.
- ACI Committee 209.** (1978): Prediction of creep, shrinkage and temperature effects in concrete structures, Second Draft, American Concrete Institute, Detroit, October. 98.
- American Concrete Institute.** (1995): Building code requirements for structural concrete. ACI 318M-95, USA.
- Bazant, Z.P.; Cusatis, G.; Cedolin; L.** (2004). Temperature effect on concrete creep modeled by microprestress-solidification theory. *J. of Engrg. Mechanics ASCE* 130 (6) 691–699
- Bazant, Z.P.; Panula, L.** (1982): New model for practical prediction of creep and shrinkage, Publication SP-76, American Concrete Institute.
- Bazant, Z.P.; Wu, S.T.** (1974): Dirichlet series creep function for aging concrete, *J. Eng. Mech. Div. ASCE* 100 (EM3).
- Bazant, Z.P.** (1982): Mathematical models for creep and shrinkage of concrete, in: Z.P. Bazant, F.H. Wittman (Eds.), *Creep and Shrinkage in Concrete Structure*, Wiley, New York.
- Crichton, A. J.; Benzenati, I.; Qiu, T. J.; Williams, J.** (1999): Kinta RCC Dam – are over- Simplified Thermal Structural Analysis, *ANCOLD* Issue No. 115.
- Conrad, M.; Aufleger, M.; Malkawai, A.IH.** (2003): Investigations on the modulus of elasticity of young RCC. In: *Proceedings of the fourth international symposium on roller compacted concrete (RCC) dams*, pp. 729-33.
- Du, C.J.; Liu, G.T.** (1994): Numerical procedure for thermal creep stress in mass concrete structures, *Comm. Numer. Methods Eng.* 10 (1994) 545}554.
- Huang, X.** (1999): The three dimensional modelling of thermal cracks in concrete structure, *journal of materials and structures*, Vol.32, No. 1359-5997, PP. 673-678, 1999.

- Incropera, F.P.; DeWitt D.P.** (2002): *Fundamentals of heat and mass transfer*. New York: John Wiley & Sons. p. 289–96 [chapter 5].
- Jaafar, M.S.; Bayagoob, K.H.; Noorzaei, J.** (2007): Development of finite element computer code for thermal analysis of roller compacted concrete dams, *Advances in Engineering Software*. **38**(11-12), 886-895.
- Kupfer, H. B.; Gerstle, K. H.**(1973): Behavior of concrete under biaxial stresses. *J. Engng Mech. Div. ASCE* 99, 852-866 (1973).
- Malkawai, A. I.H.; Mutasher, S. A.** (2003): direct tensile strength for roller compacted (RCC) gravity dams. *In: Proceedings of the Fourth International Symposium On roller compacted concrete dams*, pp. 645-649.
- Majorana, C.E.; Zavarize, G.; Borsetto, M.; Giusepetti, M.** (1990): Nonlinear analyses of thermal stresses in mass concrete castings. *Int. J. Cem. Concr. Res.* 20 (1990), pp. 559–578
- Noorzaei, J.; Bayagoob, K.H.; Thanoon, W.A. Jaafar, M.S.** (2006): Thermal and Stress analysis of Kinta RCC dam. *Journal Engineering Structures*, Vol.28, pp. 1795–1802.
- Noorzaei, J.; Bayagoob, K.H.; Abdulrazeg, A.A.; Jaafar, M.S.; Mohammed, T.A.** (2009): Three Dimensional Nonlinear Temperature and Structural Analysis of Roller compacted Concrete Dam, *CMES: Computer Modeling in Engineering & Sciences*, vol.47, no.1, pp.43-60.
- Saetta, A.; Scotta, R.; Vitaliani, R.** (1995): Stress analysis of concrete structures subjected to variable thermal loads. *J Structural Eng ASCE*, Vol. 121, No.3, pp. 446-57.
- Santurjian, O.; Kolarow, L.** (1994): A spatial FEM model of thermal stress state of concrete blocks with creep consideration, *Computers and Structures*, Vol. 58, No. 3, pp. 563-574.
- Sergerlind, L .J.** (1984): *Applied Finite Element Analysis*. (2<sup>nd</sup> ed.). New York. John Wiley and Sons.
- SUNGAI Kinta dam RCC** (2002): Study of restrictions on RCC temperature, Stage 2 development of Ipoh water supply; Technical report GHD, SDN Bhd: Malaysia.
- Tatro, S.; Schrader, E.** (1985): Thermal Considerations for Roller Compacted Concrete, *Journal of the American Concrete Institute*, March-April, pp. 119-128.
- Westman, G.** (1999): Concrete creep and thermal stresses, *PhD thesis*, Lulea University of technology, Lulea, Sweden, 1999
- Wu, Y.; Luna, R.** (2001): Numerical Implementation of temperature and creep in mass concrete, *Journal of Finite elements analysis and design*, Vol.37, PP.97-106.

**Yuan, Y.; Wan, L.** (2002): prediction of cracking within early-age concrete due to thermal, drying and creep behavior, *Journal of cement and concrete research*, Vol.32, PP.1053-1059.

**Zhang, G.; Zhu, B.** (2003): Thermal stress simulation and possible crack analysis of Mianhantan RCC dam, *Proceedings of the Fourth International Symposium on RCC Dams*, Madrid, Spain. pp. 603-609.

**Zhu, B. F.; Wang, T. S.; Ding, B. Y.** (1976): Thermal Stresses and Temperature Control in Hydraulic Concrete Structures, (in Chinese), *Water Power Press*, Beijing.

**Zdir, M.; Ouezdou, M. B.; Neji, J.** (2008): Theoretical and experimental study of roller-compacted concrete strength, *Journal of Concrete research*, vol.60, no.7, pp. 469-474.

**Zhang, M. L.** (1995): Study on structural treatment, stress and stability of roller compacted concrete gravity dam, Master's Thesis, Department of Hydraulic and Hydropower Engineering, Tsinghua University, Beijing, China.